The Correction of EPI-induced Geometric Distortions and Their Evaluation

*Guozhi Tao, Renjie He, Aziz H. Poonawalla, and Ponnada A. Narayana**

Department of Diagnostic and Interventional Imaging, University of Texas Medical School at Houston, 6431 Fannin, Houston, TX 77030.

ABSTRACT

An algorithm for correcting the geometric distortions in the echo planar images and diffusion weighted images is described. In this method the geometric distortion in the echo planar imaging (EPI) data is corrected by non-rigid registration to conventional fast-spin echo (FSE) images. The registration is based on a variant of the Demon's algorithm [10] with consistency enforced by an improved bijectivity scheme. Quantitative metrics based on the forward similarity and inverse consistency measures, calculated from the closest point distances of the image contours, are used to evaluate the performance of nonlinear registration algorithms. The experimental results demonstrated that the proposed nonlinear registration algorithm is able to correct large distortion in the EPI and diffusion weighted images (DWI) while preserving the topology of brain structure.

Index Terms— Image registration, Magnetic resonance imaging.

1. INTRODUCTION

Advanced MRI techniques such as diffusion tensor imaging and functional MRI require fast imaging sequences such as EPI. However, these fast sequences are very susceptible to local magnetic field inhomogeneities that cause significant geometrical distortion, which must be corrected for a meaningful interpretation of the data [9]. Earlier efforts to correct these distortions mainly focused on modifying the image acquisition schemes such as using spatially-tailored pulse sequences [1, 13] and utilize deformation maps obtained from phantom images [4, 7]. More recent studies on distortion correction are based on nonlinear image registration of the EPI images to anatomical MR images acquired using slow imaging sequences [2, 6, 8, 11]. One of the more recent reports on EPI distortion correction used the optical flow based nonlinear registration method [2]. Since EPI images suffer from local distortions, global measures for evaluating the quality of registration may be inappropriate.

In these studies we will employ a variant of Demon's algorithm [10] by dense mapping and with an improved method for voxel adaptive regularization. We present an improved bijectivity scheme to gurantee invertability of the nonlinear registration that performs better than Demon's original bijectivity strategy [12]. Elastic constraint driven by local correlation ratio (LCR) is developed to spatially adjust the strength of elasticity. The performance of the registration algorithm under different elastic constraints is carefully investigated. We have developed metrics for quantitative evaluation of the performance of the distortion correction algorithm. These metrics are based on the feature point (image contour) extracted from the EPI and FSE images.

2. METHOD

2.1. Viscoelastic Nonlinear Registration

Given two image volumes, a target volume I and a source volume J, we want to determine the deformation $T: J \to I$. T is represented by the displacement field $U(p)$ for each voxel p of the target image such that $T(p) = p + U(p)$. Therefore, a voxel p with intensity $I(p)$ in the target image corresponds to a point $T(p)$ with intensity $J(p+U(p))$ in the source image. $J(p+U(p))$ is denoted by $(J \circ U)(p)$. The cost function is then given as [10]:

$$E = SSD(I, J \circ U) + \beta \sum_{\alpha \in \{x,y,z\}} \int [1 - c(x,y,z)] \left\| \nabla \frac{\partial U_\alpha}{\partial t} \right\| + \gamma \sum_{\alpha \in \{x,y,z\}} \int s(x,y,z) \left\| \nabla U_\alpha \right\| \quad (1)$$

where the first term is the similarity measure based on sum of squared difference (SSD), the second term is a term for viscous regularization and the third term is for elastic regularization. In Equation (1), 1-$c(x,y,z)$ denotes the strength of the viscous constraint, $s(x,y,z)$ denotes the strength of the elastic constraint, and $\frac{\partial U_\alpha}{\partial t}$ denotes the correction field. The constants β and γ control the balance. The first term is minimized by gradient descent and the regularization terms (terms 2 and 3) are minimized separately through diffusion process that can be solved efficiently by the Additive Operator Scheme (AOS) [14]. Composite strategy is used to update the displacement field for correcting large deformations [10].

*ponnada.a.narayana@uth.tmc.edu. This work is supported by the National Institutes of Health Grant EB002095

2.2. Improved Bijectivity Scheme for Consistent Registration

To keep the topology of brain during the deformation, the transform must be consistent or bijective to guarantee the invertability. The bijectivity scheme used in the original Demon's algorithm is to iteratively estimate the forward transformation T_{12} on the grid point of image *I*, reverse transformation T_{21} on the grid points of image *J*, and residual transformation *R* on the grid points of image *I* by composing the transformation T_{12} and float transformation T_{21}. Half of the residual is added to the forward deformation field and half of the residual is mapped through the backward deformation to the grid points of image *J* by interpolating the residual field *R* and add to the backward transformation T_{21}.

Instead of calculating the residual field for a single image and mapping it to another image, we also calculated the residual field R' on the grid points of image *J* using the same idea for calculating the residual field *R*. This strategy would avoid error propagation in mapping *R* back to the grid point on another image.

2.3. Voxel Level Adaptive Regularization:

Most of the techniques proposed so far for non-rigid registration uniformly impose constraints over the entire image domain or impose elastic constraint by the tissue types. The deformation field for registering EPI and FSE images should vary spatially based on the local magnetic field gradients and not on the tissue type. We address this spatially varying elastic constraint by calculating the local correlation map between the source image and the target image, and use the local correlation value as the elastic constraint $s(x, y, z)$ for each voxel. This local correlation map driven elastic constraint method should be able to register any intra-subject registration with large local distortion. For improved computational efficiency, we calculated the local correlation ratio using a Gaussian window instead of a hard block [3].

3. QUANTITATIVE METRICS BASED ON THE CLOSEST POINT DISTANCES:

We developed quantitative metrics based on the distances of the closest points between the image pair to evaluate the registration results. The performance of our nonlinear registration algorithm is evaluated from two aspects: 1) forward similarity metric that measures the similarity between the deformed source image (EPI) and the target image (FSE), and 2) inverse consistency metric that measures the similarity between the source image and inverse deformation of the deformed source image. The inverse deformation is calculated explicitly by the iterative method proposed by Chirsten [5].

Feature points in the target image (FSE) are defined by $\{x_i\}_{i=1:N_1}$, where N_1 is the number of contour points in the target image. Feature points in deformed source image are defined as $\{y_j\}_{j=1:N_2}$, where N_2 is the number of contour points in the deformed source image. For each point x_i, we find the point $y_{ci} = \arg\min_{j=1:N2} \| y_j - x_i \|$ that is closest to point x_i in $\{y_j\}_{j=1:N_2}$. We then compute the distances $\{d_i\}_{i=1:N1}$, where $d_i = \|x_i - y_{ci}\|$ are defined on the target image to measure the forward similarity between the target image and the deformed source image. The closest point distances defined on the source image can be used to obtain the similarity between the source image and inverse deformation of deformed source image to measure the inverse consistency.

We tested the performance of our algorithm on EPI, FSE, diffusion weighted images acquired on ten normal subjects. All images were acquired on a 3T Philips scanner. The effect of proposed bijectivity scheme and the role of elastic constraint on registration were evaluated by comparing the registration results with and without bijectivity scheme under different levels of uniformly elastic strength varying from 0 to 1. The viscoelastic registration algorithm with bijectivity scheme and elastic constraint driven by local correlation ratio was also tested. The performance of our registration algorithms is compared with the results obtained with the freely available image registration tool AIR 5.2 with 30 parameters 2nd order 3D model and 1365 parameters 12th order 3D model [15].

4. RESULTS

Figure 1 shows the evaluation results obtained on ten subjects for both forward similarity (Fig. 1a) and backward inverse consistency (Fig. 1b) metrics. The mean value of *di* was used to measure the similarity. The points and error bars in these plots represent the mean and standard deviation over all the ten subjects. As seen in Figure 1a, the forward similarity metric consistently shows that all the viscoelastic registration methods produced lower mean value of d_i compared to the 2nd order and the 12th order AIR. The AIR algorithm using 1365 parameters produced higher forward similarity metric than the AIR algorithm using only 30 parameters. The performance of the Viscoelastic registration with bijectivity scheme provided superior results compared to the corresponding methods without bijectivity scheme, not only on forward similarity

metrics (Fig. 1a), but also on the backward inverse consistency metrics(Fig. 1b).

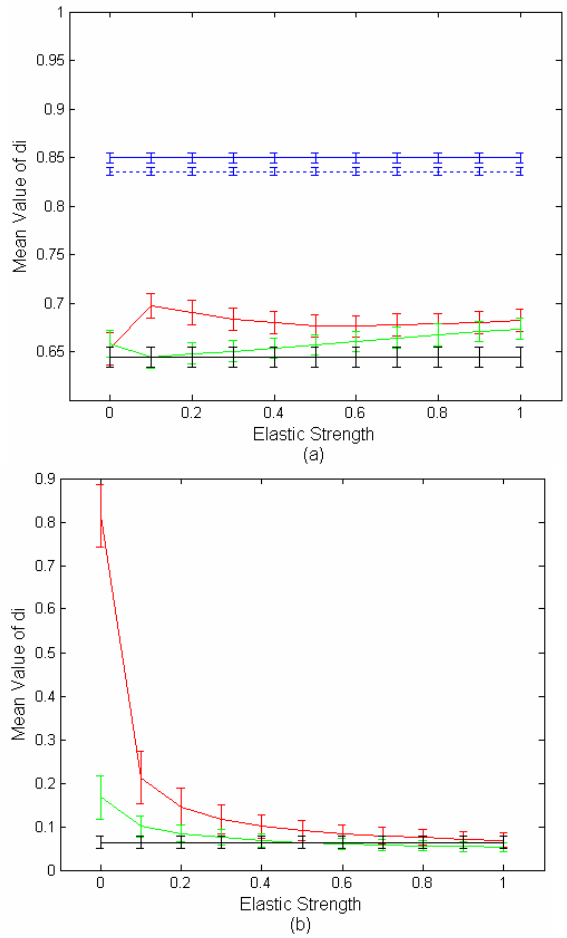

Figure 1: Comparison of the forward similarity (a) and the inverse consistency (b) of nonlinear registration algorithms, Solid blue: AIR 2nd order of 3D nonlinear model with 30 parameters; Dashed blue: AIR 12th order 3D nonlinear model with 1365 parameters, Red: Viscoelastic registration without bijective scheme; Green: Viscoelastic registration with bijective scheme; Black: Viscoelastic registration with bijective scheme. The results are based on the mean value of *di* on ten subjects. The standard deviation in Figure 1 (a) is rescaled to 1/3 for visual clarity.

Viscoelastic registration with bijectivity scheme and with local correlation ratio driven elastic constraint produced registration results with higher forward similarity than all the other methods. These results also demonstrate that values of inverse consistency metrics approach the value of bijective registration method when the elastic strength closes to one.

The distortion correction results produced by the viscoelastic registration algorithm with bijectivity scheme and elastic constraint driven by LCR and AIR (12^{th} order 3D model) are visually compared by superimposing the contour of the FSE image on the corresponding EPI image. Figure 2 shows the registration results of selected slices where the distortions (particularly the frontal and temporal lobes) are large. As can be seen from this figure, AIR produced poor registration result at both selected slices. At

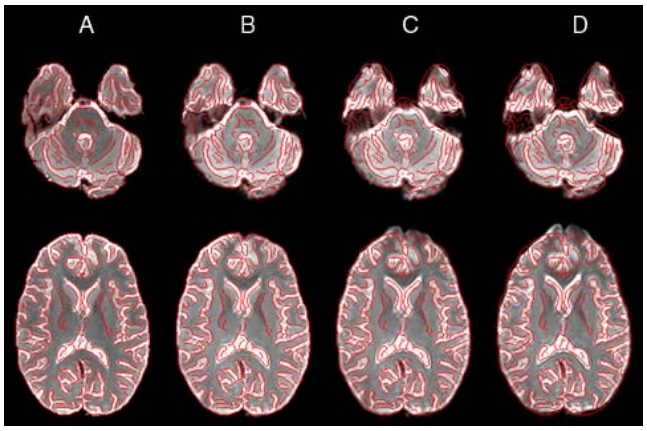

Figure 2: Visual evaluation the performance of the distortion correction on the single shot EPI images at the level of temporal lobes (top) and lateral ventricles (bottom). The FSE images along with contours are shown in (A). Superposition of contours on (B) distortion corrected EPI images using our algorithm, (C) corrected EPI image with AIR 12^{th} order nonlinear 3D model with 1365 parameter and (D) the original uncorrected EPI image. The slice thickness of the images is 3 mm.

the front lobes of the brain where the distortions are large, our algorithm performed very well while AIR only marginally reduced the distortions.

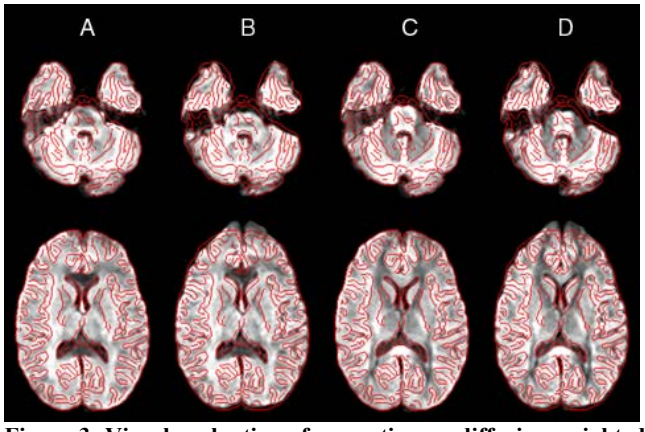

Figure 3: Visual evaluation of correction on diffusion weighted EPI images acquired at two levels of brain with $b = 1000 s/mm^2$. (A) DWI (with diffusion gradient along anterior-posterior direction) after distortion correction, (B) before distortion correction, (C) DWI (with gradient direction along left-right direction) after distortion correction, and (D) before distortion correction.

We applied our technique to correct for the geometric distortions due to the gradient induced eddy currents in DWI. Figure 3 shows the selected slices of DWI. Based on

these images, the proposed algorithm corrected the large distortion seen in DWI also.

5. CONCLUSIONS

In this paper, we implemented a nonlinear registration algorithm to correct the geometric distortions in EPI images by registering to anatomical FSE images. The consistency of the registration is enforced by an improved bijectivity scheme. We also used local correlation ratio to drive the elastic constraint for adaptively adjusting the elastic constraint. The role of elastic strength and bijectivity scheme in nonlinear registration is also investigated.

Metrics based on the closest point distances are developed to quantitatively evaluate the performance of our nonlinear registration algorithm. The quantitative metrics are used not only to quantify the quality of the registration in term of forward similarity-similarity between the target image and the deformed source image but also used to measure the inverse consistency of the registration. The proposed metrics concentrate only on the structures of the image thus we believe our proposed metrics can provide more meaningful evaluation compared to other currently used. Both quantitative analysis and visual inspection results demonstrate the proposed LCR driven elastic registration algorithm with bijectivity scheme produced the best registration results.

REFERENCE

[1] A.L. Alexander, J.S. Tsuruda, and D.L. Parker, "Elimination of eddy current artifacts in diffusion-weighted echo-planar images: The use of bipolar gradients," *Magn. Reson. Med.*, vol.38, no.6, pp.1016–1021, 1997.

[2] S. Ardekani, and U. Sinha, "Geometric distortion correction of high-resolution 3T diffusion tensor brain images," *Magn. Reson. Med.*, vol. 54, pp.1163–1171, 2005.

[3] Cachier P, Pennec X. 3D Non-Rigid Registration by gradient descent on a gaussian-windowed similarity measure using convolutions**.** *In* Proc. of IEEE Workshop on Mathematical Methods in Biomedical Image Analysis. pp. 182-189, 2000.

[4] H. Chang, and J.M. Fitzpatrick, "A technique for accurate magnetic resonance imaging in the presence of field inhomogeneities," *IEEE Trans. on Med. Imag.*, vol. 11, pp. 319–329, 1992.

[5] G.E. Christensen, and H.J. Johnson, "Consistent image registration," *IEEE Trans. on Med. Imag.*, vol. 20, no. 7, pp. 568-582, 2002.

[6] P. Hellier, and C. Barillot, "Multimodal non-rigid warping for correction of distortions in functional MRI," *Proceedings of the Third International Conference on Medical Image Computing and Computer-Assisted Intervention*, pp. 512-520, 2000.

[7] P. Jezzard, and R.S. Balaban, "Correction for geometric distortion in echo planar images from B field variations," *Magn. Reson. Med.*, vol. 34, pp.65-73, 1995.

[8] J. Kybic, A. Nirkko, and M. Unser, "Unwarping of unidirectionally distorted EPI images," *IEEE Trans. on Med. Imag.*, vol. 19, pp. 80-93, 2000.

[9] T. Netsch, and A.V. Muiswinkel, "Quantitative evaluation of image-Based distortion correction in diffusion tensor imaging," *IEEE Trans. on Med. Imag.*, vol.23, pp. 789-798, 2004.

[10] R. Stefanescu, X. Pennec, and N. Ayache, "Grid powered nonlinear image registration with locally adaptive regularization," *Medical Image Analysis*, vol.8, no.3, pp. 325-342, 2004.

[11] C. Studholme, R.T. Constable, and T.S. Duncan, "Accurate alignment of functional EPI data to anatomical MRI using a physics-based distortion model," *IEEE Trans. on Med. Imag.*, vol.19, pp. 1115–1127, 2000.

[12] J.P. Thirion, "Image matching as diffusion process: an analogy with Maxwell's demons," *Medical Image Analysis*, vol. 2, no.3, pp.243-260, 1998.

[13] X. Wan, G.T. Gullberg, D.L. Parker, and G.L. Zeng, "Reduction of geometric and intensity distortion in echo-planar imaging using a multi-reference scan," *Magn. Reson. Med*, vol.37, no.6, pp. 932-942, 1997.

[14] J. Weickert, B. Haar, and R. Viergever, "Efficient and reliable schemes for nonlinear diffusion filtering," *IEEE Trans. on Image Processing*, vol. 7, pp.398-410, 1998.

[15] R.P. Woods, S.T. Grafton, C.J. Holmes, S.R. Cherry, and J.CMazziotta, "Automated image registration: I. General methods and intrasubject, intramodality validation," *Journal of Computer Assisted Tomography*, vol. 22, pp.139-152, 1998.